

# Feature Extraction of MRI Brain Images for the Early Detection of Alzheimer's Disease

Sandeep C. S.<sup>1,\*</sup>, Sukesh Kumar A.<sup>1</sup>, K. Mahadevan<sup>2</sup>, Manoj P.<sup>3</sup>

<sup>1</sup>Department of ECE, College of Engineering University of Kerala, Trivandrum, India

<sup>2</sup>Department of Ophthalmology, Sree Gokulam Medical College, Trivandrum, India

<sup>3</sup>Department of Neurology, Sree Gokulam Medical College, Trivandrum, India

## Email address:

sandeepcs07nta@gmail.com (Sandeep C. S.), drsukeshkumar@yahoo.in (Sukesh K. A.)

\*Corresponding author

## To cite this article:

Sandeep C. S., Sukesh Kumar A., K. Mahadevan, Manoj P. Feature Extraction of MRI Brain Images for the Early Detection of Alzheimer's Disease. *Bioprocess Engineering*. Vol. 1, No. 2, 2017, pp. 35-42. doi: 10.11648/j.be.20170102.11

**Received:** April 9, 2017; **Accepted:** May 2, 2017; **Published:** June 26, 2017

---

**Abstract:** Alzheimer's disease (AD) is a common form of senile dementia. Although the understanding of key steps underlying neurodegeneration in Alzheimer's disease (AD) is incomplete, it is clear that it begins long before symptoms are noticed by patient. Conventional clinical decision making systems are more manual in nature and ultimate conclusion in terms of exact diagnosis is remote. In this case, the employment of advanced Biomedical Engineering Technology will definitely helpful for making diagnosis. Any disease modifying treatments which are developed are most possibly to be achieving success if initiated early in the process, and this needs that we tend to develop reliable, validated and economical ways to diagnose Alzheimer's kind pathology. However, despite comprehensive searches, no single test has shown adequate sensitivity and specificity, and it is likely that a combination will be needed. Profiling of human body parameter using computers can be utilised for the early diagnosis of Alzheimer's disease. There are several imaging techniques used in clinical practice for the diagnosis of Alzheimer's type pathology. There are lot of tests and neuroimaging modalities to be performed for an effective diagnosis of the disease. Prominent of them are Magnetic Resonance Imaging Scan (MRI), Positron Emission Tomography (PET), Single Photon Emission CT Scanning (SPECT), MRI Imaging and Optical Coherence Tomography (OCT). In this research we have proposed a new scheme based on Wavelet Networks (WN) for the feature extraction of MRI brain images for the early diagnosis of AD. The database of MRI images were obtained from Sree Gokulam Medical College and Research Foundation (SGMC&RF), Trivandrum, India.

**Keywords:** Alzheimer Disease, Dementia, Wavelet Networks, Sombrero, MRI Image, Early Diagnosis

---

## 1. Introduction

Alzheimer's disease (AD) is a progressive deteriorating and loss function of the neurons in the human brain. It leads to loss of memory of the subject and weakens the proficiency in doing a sequence of actions regularly following [1, 2]. AD is the sixth-leading cause of death among various diseases and is 70% widespread in all cases of dementia [6]. According to another report every 71 sec, someone develops Alzheimer's disease and the rate doubles roughly every 10 years after age 65 [7]. Some studies show that almost 36 million people are believed to be living with Alzheimer's disease and other types of dementias. This will increase to about 66 million by 2030 and nearly 115 million by 2050 [8].

The development of AD can be placed into four stages. The first stage is called Mild Cognitive Impairment (MCI) that does not make prominent changes in day to day living. The second and third stages of the disease are called as Mild and Moderate AD. These stages describe the distinctive nature by a rise in cognitive shortfall, and reduction in independence. The fourth stage is called Severe AD in which the affected person almost dependent on caregivers and an overall decline of personality [9]. Alzheimer's disease is one of the underlying causes of dementia, the term used to point out weakened brain functions and related symptoms like difficulty in performing routine tasks, memory loss, confusion, loss of intellectual functions and poor judgment. The above mentioned conditions are similar symptoms of

below mentioned neurological disarrays. This includes Alzheimer's disease, Frontotemporal Dementia, vascular dementia, Dementia with Lewy Bodies and Parkinson's disease. AD is the most common type of dementia and is clinically evident when there is gradual loss of brain functions. The symptoms thus occurring may lead to disorientation and aphasia (difficulty in language), indicating cortical dysfunction, agnosia (impairment in recognizing object and people), apraxia (impaired motor function) and significant of all, memory impairment. As the disease develops drastically, the patients suffer disability and immobility. The brain of such patients shows gross cortical atrophy with ventricular enlargement. The most widely known neuropathological hallmarks of AD are senile plaques which are seen outside the neuron and neurofibrillary tangles that are seen inside the neuron. Neurofibrillary tangles are filamentous bundles in cytoplasm of the neurons displacing or encompassing nucleus. In the pyramidal cells, they appear as 'flame' while in rounder cells they appear as 'globos tangles' [10]. Senile plaques present outside the neuron, appear as spherical bodies bearing dilated and tortuous neuritic processes around an amyloid beta core which contains some abnormal proteins like amyloid beta plaques which are derived through the processing of Amyloid Precursor Protein (APP) [10, 11]. Familial causes or genetic reasons involved in disease pathology include mutations on chromosomes 21, 14 and 1. Risk factors for AD are elder age, small head size, history of head trauma, lower intelligence, and female gender [12, 13].

The imaging modalities tests that were established for AD are Computed Tomography (CT), Magnetic Resonance Imaging (MRI), Positron Emission Tomography and neuropsychological tests. CT scans were used to check for structural deterioration of the brain and increased ventricle size. It was noticed that at firstly cerebral atrophy was predominant in AD patients than control subject. However it was discovered later that healthy people also have cerebral atrophy. Patients with dementia may not have cerebral atrophy at least in the early stages of the disease. From these findings it was difficult to distinguish between a healthy elderly patient and a patient with dementia. So the CT scans have been deemed as clinically not as useful in the primary diagnosis of AD. After CT structural MRI was introduced to evaluate MCI (mild cognitive impairment) to AD in addition to clinical measures. Structural MRI measures the whole brain volumes, medial temporal lobe structures, and ventricular volumes. Therefore MRI can be helpful in differentiating between MCI and AD [14]. PET is an imaging modality that uses biochemical ways of getting images rather than structural information. Alzheimer's disease is one of the underlying causes of dementia. Dementia is the term used to indicate impaired brain functions and encompass symptoms like memory loss, confusion, difficulty in performing routine tasks, loss of intellectual functions and impaired judgment. PET technology includes the detection of photons which records the levels of radioactivity beginning from given points in time and space. Positron emitting radioisotopes are

used to generate the radioactivity [15]. PET scan measures different compounds in the brain especially the fluorodeoxyglucose (FDG) that can compete with glucose for metabolism and absorption in neurons. With AD the neurons intake of glucose and FDG becomes less. By projecting the regions of decreased FDG uptake, PET can help in the early diagnosis of AD, even in the absence of the gross structural damage detected by other imaging techniques such as CT or magnetic resonance imaging [16]. Some studies have been conducted to examine patients that are amyloid positive or amyloid negative, PET has been used extensively to study AD, and it is evolving into an effective tool for early diagnosis. PET is a very costly scan to perform the test for AD, it has been the most useful to provide visual images in the detection of the disease. There are some recent advances in technology that can not only detect AD, but it can possibly explain the symptoms and how the disease works. The neuropsychological tests are used to examine the specific type and level of cognitive impairment that the patient is having. Some of them that were, "Mini Mental State Examination, Trail Making Test parts A and B, Digit Symbol Substitution Test, Digit Span forward and backward, Rey Auditory Verbal Learning Test, category fluency, and the Clock Drawing task" [13]. All of these tests are helpful in showing the memory recall of a patient and the realizable areas where the patient may degrade. Using the above different tests, it can be helpful to determine the types of treatment plans which are to be used. However neuropsychological tests alone are not helpful in detecting early AD, trials were often conducted combining neuropsychological tests with clinical tests and various imaging modalities. For an effective and early diagnosis of AD, a population based study is necessary and required, which gives an idea about the various tests involved in determining AD [14-16].

Preprocessing is by using median filter which removes unwanted noises on the obtained MRI image of the brain. For the different steps involved in MRI image analysis of brain, segmentation is the most important stage of all. Image segmentation is defined as the process of partitioning a digital image into multiple segments. The goal of segmentation is to simplify and/or change the representation of an image into something that is more meaningful and easier to analyze. Image segmentation is mostly used to locate objects and boundaries like lines, curves etc. in images. More accurately, image segmentation is the process of assigning a label to every pixel in a digital image such that pixels with the same label share certain visual characteristics. The result of image segmentation is a set of segments that collectively cover the whole image, or a set of contours extracted from the image. Each of the pixels in a region is similar with respect to some characteristics such as color, intensity, or texture. There are different ways for the segmentation of images in the artificial intelligence field. Most prominent and popular of them are fuzzy logic and artificial neural network (ANN) approaches for segmentation of medical images [17, 18]. Apart from above another

promising computational intelligence method that has been widely used for various applications in different areas is wavelet network (WN). A wavelet can be called as a wavelike oscillation with amplitude that begins at zero, increases, and then decreases back to zero. A family of wavelet scan is formed from a function, called "mother wavelet," which is confined in a finite interval. "Daughter wavelets" are then formed by shifting and scaling of mother wavelet. Wavelets are mainly useful for compressing image data from a larger one. Wavelet network takes full advantage of the characteristics of denoising, background reduction, and recovery of the characteristic information and Neural Network capacity of universal approximation [19-22]. For this reason, it has a great ability to be used in many different applications [23, 24]. For instance, in image processing wavelet networks have overcome many of the limitations in other intelligent methods such as artificial Neural Networks. The main advantage of wavelet networks over similar architectures such as multilayer perceptrons (MLP) and networks of radial basis functions (RBF) is the possibility of optimizing the wavelet network structure by means of efficient deterministic construction algorithms [25]. In this paper a specific wavelet network for segmentation of MRI images is employed. Wavelet networks are classified into two groups. They are adaptive wavelet networks (AWNs) and fixed-grid wavelet networks (FGWNs) [26]. Adaptive wavelet network is continuous wavelet transform whereas FGWN is discrete wavelet transform. Due to numerous shortcomings of AWNs like for example, complex calculations, sensitivity to initial values, and the problem of measuring initial values, their application is limited [29]. In an FGWN, the outer parameters of the network like number of wavelets, scale, and shift parameters value are determined. The only inner parameters of the network, weights are specified by algorithms similar to the least squares. These types of networks do not need training. In AWNs, initial values of network parameters including weights of neurons, shifts, and scales of wavelets are selected randomly or using other methods. These parameters are then updated in the training stage by means of techniques such as gradient descent or back propagation (BP). Then, the optimized values of network parameters are calculated. But in an FGWN, the number of wavelets, as well as the scale and shift parameters, can be determined in advance and the only unknown parameters are the weight coefficients which are calculated through methods such as least squares. So in proposed FGWN, there is no need to specify random initial values for parameters or to use gradient descent, BP, or other iterative methods. Normally, in training stage of an adaptive network, all the parameters change; on contrary, in FGWN only, the weights are specified during an on iterative process. Thus, it could be concluded that FGWNs do not need training procedure. A three-layer FGWN with one hidden layer is employed Specific wavelet network or MRI image segmentation as shown in figure 2. The procedure for image segmentation in this paper is as follows. At first the input data are normalized. Then, after selecting a proper mother

wavelet, which is usually Sombrero because of its desirable characteristics such as convenient calculates on, adaptability to Gaussian structures, and robustness against noise [27]. Next a wavelet lattice is formed. Wavelet lattice is a hyper shape of shift and scale values of wavelets. The huge dimensions of this hyper shape should be decreased and effective wavelets should be selected. All of these are accomplished through two stages of screening. This paper is unique as it employs two stages of screening. This gives ground to increase the popularity of the wavelet lattice and to estimate the function in a more accurate way which is most beneficial and significant for larger scales. The feature extraction step is added to improve the accuracy of diagnosis. The author's previous works in the area of Biomedical Engineering will definitely help to develop a new proposed tool using latest biomedical methods for the solution of the early diagnosis of AD [1-5]. The organization of this paper is as follows: The basic concept of WN is introduced in Section 2. In this section, the WN structure with the algorithm necessary for formation of network and determination of its parameters is presented. In Section 3, the proposed segmentation process based on WN is introduced. In Section 4, the proposed feature extraction process is introduced. The simulation results of the proposed method in comparison with other approaches are illustrated in Section 5. In Section 6, a summary and conclusion of the findings of the study is presented and finally in section 7, limitations and future expansion is discussed.

## 2. Concepts of Wavelet Networks

### 2.1. Structure of Wavelet Network

The output signal of a wavelet network with one output  $f$ ,  $d$  inputs and  $q$  wavelons (wavelet neurons) in the hidden layer is given by the equation (1).

$$\sum_{i=1}^n w_i \psi_{p_i, q_i}(X) = \sum_{i=1}^n w_i 2^{-p_i d/2} \psi(2^{p_i} X - q_i) \quad (1)$$

where  $w_i$ ,  $i = 1, 2, \dots, n$ , are weight coefficients,  $\psi_{p_i, q_i}$  are dilated and translated versions of a mother wavelet function,  $\psi$  and  $p_i, q_i$  are scale and shift parameters, respectively [25]. A three-layered WN structure with one hidden layer is shown in figure 1.

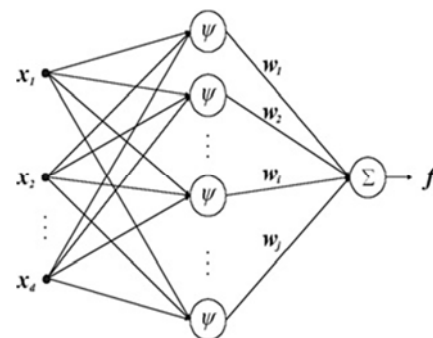


Figure 1. Three-layered WN structure with one hidden layer.

## 2.2. Algorithm for Building an FGWN

A major advantage of wavelet networks over other neural architectures is the availability of efficient construction algorithms for defining the network structure [28]. In FGWN, after determining the structure, the weights  $w_i$  in equation (1) can be obtained through linear estimation techniques. In this study, a constructive method is employed to build an FGWN. Suppose there are  $P$  input-output data in the form  $\{x^{(k)}, f^{(k)}, k=1, 2, \dots, P\}$  where  $X^{(k)}$  is the input  $d$ -dimensional vector and inputs matrix is the form  $X = [X^{(1)} \dots X^{(k)} \dots X^{(P)}]$ .

## 2.3. Normalization

In many cases, input data of wavelet network vary within a wide range and this variability reduces the efficiency of wavelet network. Thus, this first stage is considered as the data pre processing stage in which the input data are normalized to a certain range in order to avoid data scattering. Here the values of R, G, and B matrices of each colour MRI image are mapped into  $[0, 1]$  range by performing normalization [29] process using the equation (2).

$$x_{n,new}^{(k)} = \frac{x_{n,old}^{(k)} - t_k}{T_k - t_k} \quad (2)$$

where  $x_{n,new}^{(k)}$  is the value of each colour matrix after normalization (located in  $[0, 1]$  range), and  $t_k$  and  $T_k$  are minimum and maximum values of these matrices, respectively.

## 2.4. Selecting the Mother Wavelet

Due to better regularities and also the ease of frame generation, multi dimensional single scaling wavelet frame is employed. Here  $d$ -dimensional Sombrieradial wavelet [30] is used to implement WN. It is expressed as in equation (3)

$$\psi(x) = \eta \|x\| = (d - \|x\|^2) e^{-\|x\|^2} \quad (3)$$

## 2.5. Choose the Scale and Shift Parameters

In this stage, minimum and maximum scale levels in the form  $[p_{\min}, p_{\max}]$  and shift parameter are to be employed.

## 2.6. Formation of Wavelet Lattice

In this step regarding a hypershape on the wavelet parameters space that was selected in the previous stage, wavelet function is calculated as in equation (4) for all input vectors:

$$\psi_{pi,qj}(x) = 2^{-p_i d/2} \psi(2^{p_i} x - q_j) \quad (4)$$

where  $i=1, \dots, p_{\max} - p_{\min} + 1$ . In this equation  $\psi_{pi,qj}(x)$  is calculated by (6). The spatial figure is called wavelet lattice.

## 2.7. Primary Screening

In this stage, for every scale level selected in stage 4,  $I_k$  set

is formed for each input vector.

## 2.8. Secondary Screening

In this stage, the shift and scale parameters of wavelets that are selected in at least two set of the sets in the above section 2.5 are determined and set I is formed

## 2.9. Formation of Wavelet Matrix

Suppose that the number of selected wavelets in the last stage as  $L$ . In addition, to make the writing simpler, the couple index of  $(p, q)$  is replaced with single index of  $\{m=1, \dots, M\}$ . In this stage,  $W_{p \times M} = [\psi_1, \dots, \psi_l, \dots, \psi_M]$  matrix is calculated for all the input vectors as in equation (5) and for all the selected shift and scale parameters that are in set I.

$$W = \begin{bmatrix} \psi_1(x^{(1)}) & \dots & \psi_M(x^{(1)}) \\ \psi_1(x^{(2)}) & \dots & \psi_M(x^{(2)}) \\ \dots & \dots & \dots \\ \psi_1(x^{(P)}) & \dots & \psi_M(x^{(P)}) \end{bmatrix} \quad (5)$$

The nodes with red and blue circles are the members of sets in stage5, respectively, and the nodes with circles in both red and blue colors are the members of set I.

## 2.10. Performing Orthogonal Least Square (OLS) Algorithm

After two stages of screening, some of matrix members are still redundant. There as on is that only the input in formation and not the output information is taken into account for forming the wavelet matrix. A fast and efficient model structure determination approach has been implemented using the OLS algorithm. This approach has been extensively studied and widely applied in nonlinear system identification [25]. According to the OLS algorithm, to select the best subset of  $W$ , assuming that the size of this subset is known and denoted as  $s$ , the following steps should be taken. At first, the most significant wavelets in  $W$  is selected. Next, all other (not selected) wavelets are made orthogonal to the selected one. In the second step of the algorithm, the most significant of the remaining wavelets is again selected; then in this step, all non selected wavelets are made orthogonal with respect to the selected one, so that second selected wavelet with addition to the first one can determine the best approximation. And then, the algorithm goes on for the rest of wavelets. Since all remaining wavelets are made orthogonal to all selected ones in each step of the algorithm, the improvement of each selectable wavelet is isolated [31]. After employing this stage, wavelet network is constructed as in equation (6).

$$f = \sum_{i=1}^s w_i \psi_i(x) \quad (6)$$

Where  $s$  is the number of wavelons in the hidden layer and

wi is the weight of wave l on s. After performing the OLS algorithm, W is composed of ortho normal matrix N and upper triangular matrix A. So the above equation can be rewritten as in equation (7):

$$f = QA\theta \tag{7}$$

**2.11. Selecting the Number of Wavelons**

Wavelons are the nodes creating the hidden layer of the wavelet network. By choosing the ideal number of wavelons [35], index is calculated as in equation (8).

$$MSE = \frac{1}{P} \sum_{k=1}^P (\hat{f}^{(k)} - f^{(k)})^2 \tag{8}$$

Then, the number of wavelons will change until the desired error measure is achieved.

**2.12. Calculating Wavelons Weight Coefficient**

This stage is the last stage of the algorithm. The weight of wavelons is measured by the least-squares method. This is done by the following equation (9).

$$N^T f = A\theta \tag{9}$$

**3. Segmentation Algorithm**

The algorithm from the previous stage is used in the present stage for segmentation of the brain MRI images. From images database, a number of images are randomly chosen for formation of FGWN. At first the values of R, G, and B matrices of each colour MRI image are mapped into [0, 1] range by performing normalization process. FGWN is formed with three inputs, a hidden layer, and an output. In order to form the FGWN, the values of three colour matrices are considered as network inputs. These matrices are related to the five chosen images from the selected images for segmentation. From these images, some pixels are selected randomly (ranging from 1000 to 5000 pixels for a 763x650 image). If the pixel is inside the AD region, network output will be considered as 0, and if the pixel is outside the AD region, the output will be considered as 1. In this way, the FGWN is formed. After that, the three matrices R, G, and B for each pixel is considered as FGWN inputs, and the output of FGWN is a binary image that shows the segmented of original image is shown in figure 2.

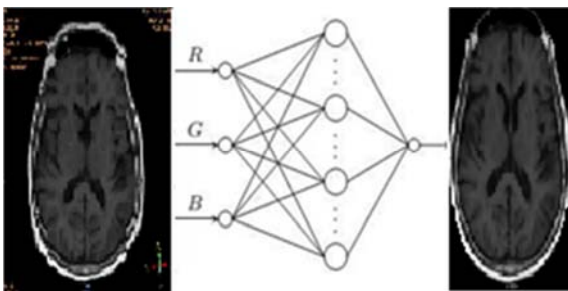


Figure 2. segmentation of MRI images.

After segmentation post processing is done. Since extracting the features of brain regions is the most essential part of diagnosing AD, extracting the exact boundary of segmented brain is a vital task. For this, after segmentation with an FGWN the space between two shapes is filled, extra parts are eliminated, and the noise is removed. Then, the exact boundary of lesion is extracted. This is done by appropriate morphological processes, including erosion, dilation [32, 33].

**4. Feature Extraction**

After the post processing is over, the next step is to extract the features of the segmented region. Feature extraction involves reducing the amount of resources required to describe a large set of data. When performing analysis of complex data one of the major problems stems from the number of variables involved. Analysis with a large number of variables generally requires a large amount of memory and computation power; also it may cause a classification algorithm to over fit to training samples and generalize poorly to new samples. Feature extraction is a general term for methods of constructing combinations of the variables to get around these problems while still describing the data with sufficient accuracy. In this proposed method, four feature extraction techniques like histogram, gradient; SURF and Gabor filter is used. They are discussed below.

**4.1. Histogram**

The histogram of a digital image is the intensity distribution of that image in a graphical form. It plots every intensity value against the number of pixels in an image. When someone watches an image histogram he will be able to identify the entire intensity distribution at a glimpse. For example, in an 8-bit gray scale digital image there are 256 different possible intensities, and so the histogram will graphically display 256 numbers showing the distribution of pixels against those gray scale values. A histogram of a digital image with gray levels in the range [1, M] is a discrete function  $f(g_k)$ , where  $g_k$  is the  $k^{th}$  gray level, and  $n_k$  is the number of pixels in the image having gray level  $g_k$ . The normalization of a histogram is done by dividing each of its value by the total number of pixels denoted by n [34] as in equation (10).

$$p(g_k) = n_k/n \text{ for } k=1, 2, \dots, M \tag{10}$$

where  $p(g_k)$  estimates the probability of occurrence of the gray level  $g_k$ . Histograms are usually used for computing a binary image  $b_{i,j}$  from a given image  $f_{i,j}$  so that  $i=1, \dots, X, j=1, \dots, Y$  where  $X, Y$  describes the size of the image in pixels ( $n=X*Y$ ). The binarization is usually done by a threshold operation. A suitable value for  $\theta$  can be found by creating a gray-level histogram as in equation (11)

$$b_{i,j} = \begin{cases} 0 & \text{if } f_{i,j} \leq \theta \\ 1 & \text{otherwise} \end{cases} \tag{11}$$

The mean of the image is calculated as as in equation (12)

$$\mu = \sum_{k=1}^M g_k P_k \quad (12)$$

Entropy is a statistical measure of randomness that can be used to characterize the texture of the input image. The entropy of a histogram (image) is as in equation (13)

$$\mu = \sum_{k=1}^M P_k \log_2 P_k \quad (13)$$

#### 4.2. Gradient

An image gradient is a directional change in the intensity or color in an image. Image gradients may be used to extract information from images. Mathematically, the gradient of a two-variable function (here the image intensity function) at each image point is a 2D vector with the components given by the derivatives in the horizontal and vertical directions. At each image point, the gradient vector points in the direction of largest possible intensity increase, and the length of the gradient vector corresponds to the rate of change in that direction [35]. The gradient of an image is given by the formula as as in equation (14)

$$\text{grad}.f = [g_x \ g_y]^T = \left[ \frac{df}{dx} \ \frac{df}{dy} \right]^T \quad (14)$$

where  $df/dx$  is the gradient in  $x$  direction and  $df/dy$  is the gradient in  $y$  direction. The gradient direction can be calculated by the formula in equation (15).

$$\theta = \tan^{-1}[g_x \ g_y]^T \quad (15)$$

#### 4.3. SURF

The SURF algorithm is based on the same principles and steps as SIFT, but details in each step are different. The algorithm has three main parts: interest point detection, local neighborhood description and matching. SURF uses square-shaped filters as an approximation of Gaussian smoothing. (The SIFT approach uses cascaded filters to detect scale-invariant characteristic points, where the difference of Gaussians (DoG) is calculated on rescaled images progressively.) Filtering the image with a square is much faster if the integral image is used [36].

$$S(x, y) = \sum_{i=0}^x \sum_{j=0}^y I(i, j) \quad (16)$$

The sum of the original image within a rectangle can be evaluated quickly using the integral image, requiring evaluations at the rectangle's four corners as in equation (16).

#### 4.4. Gabor Filter

A set of Gabor filters with different frequencies and orientations may be helpful for extracting useful features from an image. In the discrete domain, two-dimensional Gabor filters are given by the equations (17) and (18).

$$G_s[i, j] = C e^{-\frac{(i^2+j^2)}{2\sigma^2}} \sin(\omega(i\cos\theta + j\sin\theta)) \quad (17)$$

$$G_c[i, j] = B e^{-\frac{(i^2+j^2)}{2\sigma^2}} \cos(\omega(i\cos\theta + j\sin\theta)) \quad (18)$$

where B and C are normalizing factors to be determined. 2-D Gabor filters have rich applications in image especially in feature extraction for texture analysis and segmentation processing [37].

## 5. Experimental Results

### 5.1. Database

The database of MRI images was obtained from Sree Gokulam Medical College and Research Foundation (SGMC&RF), Trivandrum, India using Siemens16 channel MAGNETOM\_ESSENZA at 1.5 Tesla. This database includes different MRI images of brain taken under the same environmental conditions. All of these images are in dicom format and saved as Joint Photographic Experts Group format that are taken from patients suspected to AD, Whether or not the patients have caught the disease is determined by MRI and is diagnosed by the ophthalmologist.

### 5.2. Preprocessing

It is worth noting that the database images employed in this paper were free of any noise or artifacts. In case of noisy images (images which are not of desired quality or the results of segmentation are not satisfactory), or necessity of elimination of the hairs, a pre processing stage be used [36].

### 5.3. Results

Among the 30 images selected for segmentation and feature extraction using the proposed FGWN as diagnosed by the physician, five images having mild AD were used for building the network structure (formation of the wavelet lattice, determination of the shift and scale parameters, a calculation of the network weights), and the rest were used for testing it [2]. In our experiments, 10–12 wavelons are enough to achieve good results.

### 5.4. Post Processing

Since extracting the features of brain is the most essential part of diagnosing Alzheimer's Disease, extracting the brain layer is a vital task. For this, after segmentation with an FGWN and according to the proposed algorithm in Section 3, the space between two shapes is filled, extra parts are eliminated, and the noise is removed. Then, the exact boundary of brain layer is extracted. This is done by appropriate morphological processes, including erosion, dilation, closing and opening, and region filling. Size, shape, and kind of structuring elements were based on images dimensions and type of their objects that are selected tentatively and provisionally.

### 5.5. Evaluation of Results

As mentioned before, segmentation is the most important and critical stage of the three stages of automatic diagnosis of

brain layer which has a very significant role in the final outcome. Because of this reason, the performance of this state should be examined by means of appropriate criteria. Here the brain fibre layer which is the most significant feature in detecting Alzheimer's Disease is extracted by FGWN with an acceptable accuracy. The proposed method is quite simple and considering the satisfactory results of this study, it is very applicable for detecting AD by means of the computer or robot. The segmentation provides the necessary part of brain image and feature extraction helps to detect AD with a sub-division of improved image into constituent parts or isolation of some aspects of an image for identifying or interpreting meaningful objectforms, which includes finding lines, circles or specific shapes.

## 6. Conclusion

In this study a new approach for the segmentation of MRI brain images based on fixed grid wavelet network (WN) has been employed. A wavelet lattice is formed. Parameters of wavelets are determined with two screening stages. Orthogonal least squares algorithm is used to calculate the network weights and to optimize the network structure using the developed algorithm, hence provides a useful tool for the analysis of MRI brain images.

## 7. Limitations and Future Expansion

From the existing work a segmented image is formed; in the future works the feature extraction, feature selection and classification can be done. Feature extraction is a sub-division of improved image of improved image into constituent parts or isolation of some aspects of an image for identifying or interpreting meaningful object forms, which includes finding lines, circles or specific shapes. Later from the extracted features, best of the feature can be selected and used for classification and detection of Alzheimer's Disease.

## Acknowledgement

The authors are thankful to Sree Gokulam Medical College and Research Foundation, Trivandrum, India for providing the necessary database of brain MRI for the preparation of the paper.

## References

- [1] Sandeep C S, Sukesh Kumar A, A Review on the Early Diagnosis of Alzheimer's Disease (AD) through Different Tests, Techniques and Databases AMSE JOURNALS –2015-Series: Modelling C; Vol. 76; N° 1; pp 1-22.
- [2] Sandeep C S, Sukesh Kumar A, "A Psychometric Assessment Method for the Early Diagnosis of Alzheimer's disease", International Journal of Scientific & Engineering Research - IJSER (ISSN 2229-5518), Volume 8 Issue 3 –MARCH 2017.
- [3] Sandeep C S, Sukesh Kumar A, Susanth M J "The Early Diagnosis of Alzheimer Disease (AD) Using CAMD, TREAD and NAAC Databases" International Journal for Science and Advance Research In Technology, ISSN ONLINE 2359-1052, IJSART - Volume 3 Issue 3 –MARCH 2017: 366-371.
- [4] Sandeep C. S, Sukesh Kumar. A, "A software based on MMSE for screening the different stages of Alzheimer's Disease (AD)", ICSSP 2016, TKM Collge of Engineering.
- [5] Sandeep C. S, Sukesh Kumar. A, "A Review Paper on the Early Diagnosis of Alzheimer's Disease(AD) through Profiling of Human Body Parameters", Scientistlink, Coimbatore, India, 2013, International Journal of Computer Science and Engineering Communications (IJCEC), Vol.1 Issue.1, pp. 21-29, December 2013.
- [6] AA, 2012. Alzheimer's Facts and Figures. Alzheimer's Association.
- [7] WAD, 2011. World Alzheimer's Day on Wednesday.
- [8] ADI press release (<http://www.alz.co.uk/media/nr100921.html>) for "Alzheimer's Disease International World Alzheimer Report 2010: The Global Economic Impact of Dementia," Prof Anders Wimo, Karolinska Institutet, Stockholm, Sweden Prof Martin Prince, Institute of Psychiatry, King's College London, UK. Published by Alzheimer's Disease International (ADI) 21 September 2010.
- [9] Frosch, M. P., D. C. Anthony and U. D. Girolami, 2010. The Central Nervous System. In: Robbins and Cotran Pathologic Basis of Disease, Robbins, S. L., V. Kumar, A. K. Abbas, R. S. Cotran and N. Fausto (Eds.), Elsevier srl, Philadelphia, ISBN-10: 1416031219, pp: 1313-1317.
- [10] Harvey, R. A., P. C. Champe, B. D. Fisher, Lippincott's Illustrated Reviews: Microbiology. 2nd Edn., Lippincott Williams and Wilkins, ISBN-10: 0781782155, pp: 432, 2006.
- [11] Cummings, J. L., H. V. Vinters, G. M. Cole and Z. S. Khachaturian, Alzheimer's disease: etiologies, pathophysiology, cognitive reserve and treatment opportunities. Neurology. 51: 2-17. PMID: 9674758, 1998.
- [12] Yaari, R. and J. Corey-Bloom, Alzheimer's disease: Pathology and pathophysiology. Semin Neurol. 27: 32-41, 2007.
- [13] Larson EB, Wang L, Bowen JD, et al. Exercise is associated with reduced risk for incident dementia among persons 65 years of age and older. Ann Intern Med; 144: 73-81, 2006.
- [14] Mayeux R. Epidemiology of neurodegeneration. Annu Rev Neurosci; 26: 81-104, 2003.
- [15] Harvey RJ, Skelton-Robinson M, Rossor MN. The prevalence and causes of dementia in people under the age of 65 years. J Neurol Neurosurg Psychiatry; 74: 1206-9, 2003.
- [16] Chu LW, Tam S, Wong RL, et al. Bioavailable testosterone predicts a lower risk of Alzheimer's disease in older men. J Alzheimers Dis; 21: 1335-45, 2010.
- [17] K.-S. Cheng, J.-S. Lin, and C.-W. Mao, "Techniques and comparative analysis of neural network systems and fuzzy systems in medical image segmentation," Fuzzy Theor. Syst. Tech. Appl., vol. 3, pp. 973–1008, 1999.
- [18] J. Jiang, P. Trundle, and J. Ren, "Medical image analysis with artificial neural networks," Comput. Med. Imag. Graph., vol. 34, no. 8, pp. 617–631, Dec. 2010.

- [19] R. M. Balabin, R. Z. Safieva, and E. I. Lomakina, "Wavelet neural network (WNN) approach for calibration model building based on gasoline near infrared (NIR) spectra," *J. Chemometr. Intell. Lab. Syst.*, vol. 93, no. 1, pp. 58–62, Aug. 2008.
- [20] Q. Zhang and A. Benveniste, "Wavelet networks," *IEEE Trans. Neural Netw.*, vol. 3, no. 6, pp. 889–898, Nov. 1992.
- [21] Y. C. Pati and P. S. Krishnaprasad, "Analysis and synthesis of feedforward neural networks using discrete affinewavelet transformations," *IEEE Trans. Neur. Netw.*, vol. 4, no. 1, pp. 73–85, Jan. 1992.
- [22] H. H. Szu, B. A. Telfer, and S. L. Kadambe, "Neural network adaptive wavelets for signal representation and classification," *Opt. Eng.*, vol. 31, no. 9, pp. 1907–1916, Sep. 1992.
- [23] H. Zhang, B. Zhang, W. Huang, and Q. Tian, "Gabor wavelet associative memory for face recognition," *IEEE Trans. Neural Netw.*, vol. 16, no. 1, pp. 275–278, Jan. 2005.
- [24] O. Jemai, M. Zaied, C. B. Amar, and M. A. Alimi, "Pyramidal hybrid approach: Wavelet network with OLS algorithm-based image classification," *Int. J. Wavel. Multir. Inf. Process.*, vol. 9, no. 1, pp. 111–130, Mar. 2011.
- [25] R. Galvao, V. M. Becerra, and M. F. Calado, "Linear-wavelet networks," *Int. J. Appl. Math. Comput. Sci.*, vol. 14, no. 2, pp. 221–232, Aug. 2004.
- [26] S. A. Billings and H. L. Wei, "A new class of wavelet networks for nonlinear system identification," *IEEE Trans. Neural Netw.*, vol. 16, no. 4, pp. 862–874, Jul. 2005.
- [27] J. Gonzalez-Nuevo, F. Argueso, M. Lopez-Caniego, L. Toffolatti, J. L. Sanz, P. Vielva, and D. Herranz, "The mexican hat wavelet family. application to point source detection in CMB maps," *Mon. Not. Roy. Astron. Soc.*, vol. 369, pp. 1603–1610, 2006.
- [28] Y. Oussar and G. Dreyfus, "Initialization by selection for wavelet network training," *Neurocomputing*, vol. 34, no. 1, pp. 131–143, Sep. 2000.
- [29] R. Baron and B. Girau, "Parameterized normalization: Application to wavelet networks," in *Proc. IEEE Int. Conf. Neural Netw.*, May 1998, vol. 2, pp. 1433–1437.
- [30] Q. H. Zhang, "Using wavelet network in nonparametric estimation," *IEEE Trans. Neural Netw.*, vol. 8, no. 2, pp. 227–236, Mar. 1997.
- [31] M. Davanipoor, M. Zekri, and F. Sheikholeslam, "Fuzzy wavelet neural network with an accelerated hybrid learning algorithm," *IEEE Trans. Fuzzy Syst.*, vol. 20, no. 3, pp. 463–470, Jun. 2012.
- [32] H. Zhou, M. Chen, L. Zou, R. Gass, L. Ferris, L. Drogowski, and J. Rehg, "Spatially constrained segmentation of dermoscopy images," in *Proc. 5th IEEE Int. Symp. Biomed. Imag.: Nano Macro*, May 2008, pp. 800–803.
- [33] T. Lee, V. Ng, R. Gallagher, A. Coldman, and D. McLean, "DullRazor: A software approach to hair removal from images," *Comput. Biol. Med. Biol.*, vol. 27, no. 6, pp. 533–543, Nov. 1997.
- [34] Michael Freeman (2005). *The Digital SLR Handbook*. Ilex. ISBN 1-904705-36-7.
- [35] Korn, Theresa M.; Korn, Granino Arthur (2000). *Mathematical Handbook for Scientists and Engineers: Definitions, Theorems, and Formulas for Reference and Review*. Dover Publications. pp. 157–160. ISBN 0-486-41147-8.
- [36] Herbert Bay, Andreas Ess, Tinne Tuytelaars, Luc Van Gool "SURF: Speeded Up Robust Features", *Computer Vision and Image Understanding (CVIU)*, Vol. 110, No. 3, pp. 346–359, 2008.
- [37] Jones, J. P.; Palmer, L. A. (1987). "An evaluation of the two-dimensional gabor filter model of simple receptive fields in cat striate cortex". *J. Neurophysiol.* 58 (6): 1233–1258.